Galerkin analysis of light-induced patterns in the chlorine dioxide–iodine–malonic acid reaction-diffusion system

Pushpita Ghosh,[1] Shrabani Sen,[1] Syed Shahed Riaz,[2] and Deb Shankar Ray[1,*]
[1]*Indian Association for the Cultivation of Science, Jadavpur, Kolkata 700 032, India*
[2]*Department of Chemistry, Ramakrishna Mission Vidyamandira, Belur, Howrah 711202, India*
(Received 5 February 2009; revised manuscript received 31 March 2009; published 14 May 2009)

The photosensitive chlorine dioxide–iodine–malonic acid reaction-diffusion system has been an experimental paradigm for the study of Turing pattern over the last several years. When subjected to illumination of varied intensity by visible light the patterns undergo changes from spots to stripes, vice versa, and their mixture. We carry out a nonlinear analysis of the underlying model in terms of a Galerkin scheme with finite number of modes to explore the nature of the stability and existence of various modes responsible for the type and crossover of the light-induced patterns.

DOI: 10.1103/PhysRevE.79.056216 PACS number(s): 82.40.Bj, 82.40.Ck

I. INTRODUCTION

Pattern formation in complex biological, chemical, and hydrodynamical systems under far from equilibrium condition has been a major issue in the field of spatially extended dynamical systems [1–6]. Turing pattern [3,5,6] occupies a central place in its early development. More than half a century ago Turing showed how the interplay of reaction and diffusion of two chemical components under suitable conditions may lead to a symmetry-breaking instability of a homogeneous steady state, initiating spontaneous stationary patterns. The first unambiguous experimental evidence for convection-free Turing pattern [7] was reported in a thermodynamically open chemical system in the chlorite-iodide-malonic acid (CIMA) reaction. Since then considerable progress has been made in the experimental and theoretical studies of Turing patterns in this system and its variant [8–10], the chlorine dioxide–iodine–malonic acid (CDIMA) reaction [11].

The Turing instability is a diffusion-driven instability, which owes its origin to a competition between short-range activation and long-range inhibition of the two reacting components. Since this is intrinsic to kinetic and diffusive characteristics of the dynamical system, in question, it is difficult to manipulate the nature and type of spatial patterns. This difficulty may, however, be overcome in some cases by appropriate use of external forcing by electric and/or magnetic field, light, or suitable noise [12–34]. For example, an electric field [12–17] may affect mass transport in reaction-diffusion systems with ionic components, resulting in a symmetry-breaking instability leading to formation of stationary spatial structures or displaying varied wave-front characteristics under suitable condition. Turing-type but nonstationary patterns can be observed in polymerization reaction in acrylamide-methylene-blue-sulphide-oxygen systems [26,27] under the influence of light and electric field. Later on the methylene blue system has been further studied by Mueller and co-workers [23] to investigate pattern formation in relation to chemomechanical coupling. Spatial reorganization [35,36] has also been observed in one of the most thoroughly studied systems, the photosensitive Belousov-Zhabotinsky reaction under periodic illumination. Apart from these, noise [28–34] in both additive and multiplicative forms as well as magnetic field [18,19] have been used for inducing instabilities to generate spatial patterns in reaction-diffusion systems. A major emphasis in these studies, in general, is the exploration of a new instability condition arising out of linear stability analysis. However, several aspects remain outside the scope of linear theory. First, the nonlinearity in the dynamics leads to saturation of exponential growth of the unstable mode. Second, since the principle of superposition is not applicable, the nonlinearity may select different symmetry-adapted combinations which grow in almost competitive time scales. This results in a wide variation in the type of patterns, examples being spots, stripes, and their combinations. Under appropriate experimental conditions these patterns may undergo interesting crossover among themselves. The CDIMA reaction-diffusion system offers itself as an excellent candidate for study in this context. Because of its photosensitivity [20–22,25] the reaction is subjected to illumination by visible light, and depending on the intensity of illumination varied types of spatial patterns in the form of spots, stripes, and their mixture can be realized. At higher intensities the patterns are eliminated completely. Based on this experimental background it is worthwhile to understand the type of light-induced patterns and their crossovers. A straightforward approach to this problem is to carry out direct numerical simulations of the partial differential equations for the underlying Lengyel-Epstein model describing the CDIMA reaction-diffusion system. However, this does not throw any light on how nonlinearity gives rise to mode selection relevant for specific patterns. Since analytical solutions of the partial differential equations are practically impossible, one takes resort primarily to two analytical techniques. First, the method of amplitude equation, which can be profitably employed for weakly nonlinear systems when the spatial and temporal modulations of the basic mode are relatively slow in nature. Second one refers to Galerkin technique which involves an effective replacement of the partial differential equations for the reaction-diffusion system by a set of coupled ordinary differential equations for a few se-

*pcdsr@iacs.res.in

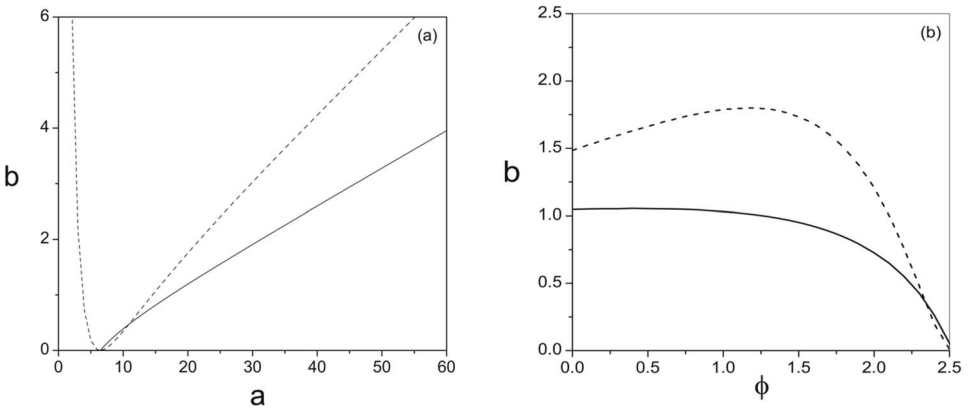

FIG. 1. Domain of Turing patterns in b vs a and b vs ϕ parameter spaces, for (a) $\sigma=9.0$ and $\phi=0.0$, and (b) $\sigma=9.0$ and $a=18.0$. The dashed line and the solid line represent the Turing and the Hopf lines, respectively.

lected modes. The classic example of using this method is the derivation of Lorenz equations for turbulence obtained from Navier-Stokes equation in hydrodynamical context. A few years back the method has been employed in the problem of pattern formation and bifurcation analysis in Geirer-Meinhardt system [37]. Marchant and co-worker [24] have considered the method for the self-replication scheme of Gray and Scott [4] to develop semianalytic technique for bifurcation analysis. Based on a finite mode Galerkin scheme we make a systematic nonlinear analysis of the reaction-diffusion system. Our aim is threefold:

(i) To envisage a Lorenz-type model for the CDIMA reaction-diffusion system.

(ii) How and to what extent this minimal Galerkin model can capture a specific class of selected modes responsible for patterns in the CDIMA system under a given set of parameter values. Furthermore, our objective is to understand how the variation in illumination intensity influences the type of patterns, transition between them, and their disappearance.

(iii) To identify and examine the conspicuous behavior of any mode(s) responsible for crossover between different types of patterns.

II. GALERKIN ANALYSIS OF THE CDIMA SYSTEM

To begin with we consider the reaction-diffusion equations [9,10,20–22,25] governing the chlorine dioxide–iodine–malonic acid reaction as given by

$$\frac{\partial u}{\partial t} = a - u - \frac{4uv}{1+u^2} - \phi + \nabla^2 u, \tag{2.1}$$

$$\frac{\partial v}{\partial t} = \sigma\left[b\left(u - \frac{uv}{1+u^2} + \phi \right) + d\nabla^2 v \right]. \tag{2.2}$$

Here "u" and "v" are dimensionless concentrations of I^- and $(ClO_2)^-$, respectively. They are dimensionless parameters. a and b are related to kinetic parameters, and are proportional to the concentration ratios $[CH_2(COOH)_2]/[ClO_2]$ and $[I_2]/[ClO_2]$, respectively, where $[ClO_2]$, $[I_2]$, and $[CH_2(COOH)_2]$ are in large excess. For further details we refer to Ref. [3]. d denotes the ratio of the diffusion coefficients, $d=[D_{ClO_2}]/[D_{I^-}]$. σ refers to the concentration of starch which forms a complex with I_3^- such that $\sigma=1+K[S]$. Here K is the equilibrium constant for the starch-iodide complex and $[S]$ is the concentration of starch tri-iodide binding sites. ϕ refers to the dimensionless rate of photochemical reaction which is proportional to the light intensity.

It is well known from the linear stability analysis [20–22,25] of the system that by varying the concentration of complexing agent (σ) one can adjust the Hopf bifurcation line in the b-a parameter plane in such a way that it lies below the Turing bifurcation line which is independent of σ, and the region of existence of Turing pattern can be realized. Figure 1(a) depicts such a region of instability. Introduction of intensity of visible light through ϕ gives a useful handle for further manipulation of the Turing space. Illumination of the CDIMA system affects both Hopf and Turing lines. By fixing "a" at an appropriate level both these lines can be suitably adjusted in b-ϕ plane so that the width of the Turing region can be widened or reduced. This is illustrated in Fig. 1(b). In conformity with this linear analysis we set the parameter values for the present problem as $a=18.0$, $b=1.5$, $\sigma=9.0$, $d=1.6$, and $k=0.1$.

While the linear analysis as summarized above allows us to identity the Hopf-Turing instability regimes in the parameter space, it does not give any clue in understanding the type of patterns and their crossovers as the illumination intensity ϕ is varied. To address this issue we take resort to nonlinear analysis of the reaction-diffusion system [Eqs. (2.1) and (2.2)] with the help of Galerkin transformation [35,36,38,39]. The idea is to understand the nonlinear interaction of a finite number of judiciously chosen modes in a Lorenz-type model. This can be achieved by approximating the two exact concentration variables u and v by a series of orthogonal basis functions. These basis functions represent the spatial structure of the concentration profile whereas the combining coefficients determine the relative weight of the profile. The dynamics of reaction-diffusion system thus reduces to nonlinear dynamics of these finite number coefficients or modes. The specificity of the nature of nonlinear interaction is expected to capture the type of spatial patterns and their crossovers.

For analysis of spots and stripes we choose specifically the following forms of expansions

$$u(x,y,t) = u_0(t) + u_{12}(t)\cos k_1 x \cos k_2 y, \tag{2.3}$$

$$v(x,y,t) = v_0(t) + v_1(t)\cos k_1 x + v_2(t)\cos k_2 y + v_{12}(t)\cos k_1 x \cos k_2 y. \quad (2.4)$$

The above choice is guided by the following consideration. For the homogeneous state, we must have $u_{12}=v_1=v_2=v_{12}=0$. For $u_{12}=v_{12}=v_2=0$ we are likely to have stripes in x direction (nodes appear only in this direction) while for $u_{12}=v_{12}=v_1=0$ we expect stripes in y direction (nodes appear only in this direction). For $v_1=v_2=0$ nodes are expected to appear in both x and y directions giving rise to spot patterns since nodes in the concentration profile can appear in both directions.

By inserting expansions (2.3) and (2.4) in Eqs. (2.1) and (2.2) with $k_1=k_2=k$ (say) and equating the coefficients of Fourier terms of both sides, we obtain the following set of equations for six coupled modes after a series of algebraic steps

$$\dot{u}_0 = a - u_0 - \frac{4}{1+u_0^2}\left[\left(u_0v_0 + \frac{u_{12}v_{12}}{4}\right)\left(1 - \frac{u_{12}^2}{4(1+u_0^2)}\right) - \frac{u_0u_{12}}{2(1+u_0^2)}(u_0v_{12} + u_{12}v_0) - \frac{5u_{12}^3v_{12}}{64(1+u_0^2)}\right] - \phi, \quad (2.5)$$

$$\dot{u}_{12} = -u_{12} - \frac{4}{1+u_0^2}\left[(u_0v_{12} + u_{12}v_0)\left(1 - \frac{u_{12}^2}{4(1+u_0^2)}\right) - \frac{5u_{12}^2}{16(1+u_0^2)}(u_0v_{12} + u_{12}v_0) - \frac{2u_0u_{12}}{(1+u_0^2)}\left(u_0v_0 + \frac{u_{12}v_{12}}{4}\right) - \frac{5u_0u_{12}^2v_{12}}{8(1+u_0^2)}\right] - 2k^2u_{12}, \quad (2.6)$$

$$\dot{v}_0 = \sigma b\left[u_0 - \frac{1}{1+u_0^2}\left\{\left(u_0v_0 + \frac{u_{12}v_{12}}{4}\right)\left(1 - \frac{u_{12}^2}{4(1+u_0^2)}\right) - \frac{u_0u_{12}}{2(1+u_0^2)}(u_0v_{12} + u_{12}v_0) - \frac{5u_{12}^3v_{12}}{64(1+u_0^2)}\right\} + \phi\right], \quad (2.7)$$

$$\dot{v}_1 = \sigma b\left[-\frac{1}{1+u_0^2}\left\{\left(u_0v_1 + \frac{u_{12}v_2}{2}\right)\left(1 - \frac{u_{12}^2}{4(1+u_0^2)}\right) - \frac{u_{12}^2}{8(1+u_0^2)}\left(u_0v_1 + \frac{u_{12}v_2}{2}\right) - \frac{3u_{12}^3v_2}{32(1+u_0^2)} - \frac{u_0u_{12}}{(1+u_0^2)}\left(u_0v_2 + \frac{u_{12}v_1}{2}\right) - \frac{u_0u_{12}^2v_1}{4(1+u_0^2)}\right\}\right] - \sigma dk^2v_1, \quad (2.8)$$

$$\dot{v}_2 = \sigma b\left[-\frac{1}{1+u_0^2}\left\{\left(u_0v_2 + \frac{u_{12}v_1}{2}\right)\left(1 - \frac{u_{12}^2}{4(1+u_0^2)}\right) - \frac{u_{12}^2}{8(1+u_0^2)}\left(u_0v_2 + \frac{u_{12}v_1}{2}\right) - \frac{3u_{12}^3v_1}{32(1+u_0^2)} - \frac{u_0u_{12}}{(1+u_0^2)}\left(u_0v_1 + \frac{u_{12}v_2}{2}\right) - \frac{u_0u_{12}^2v_2}{4(1+u_0^2)}\right\}\right] - \sigma dk^2v_2, \quad (2.9)$$

$$\dot{v}_{12} = \sigma b\left[u_{12} - \frac{1}{1+u_0^2}\left\{(u_0v_{12} + u_{12}v_0)\left(1 - \frac{u_{12}^2}{4(1+u_0^2)}\right) - \frac{5u_{12}^2}{16(1+u_0^2)}(u_0v_{12} + u_{12}v_0) - \frac{2u_0u_{12}}{(1+u_0^2)}\left(u_0v_0 + \frac{u_{12}v_{12}}{4}\right) - \frac{5u_0u_{12}^2v_{12}}{8(1+u_0^2)}\right\}\right] - 2\sigma dk^2v_{12}. \quad (2.10)$$

The dynamical equations for stripes in x direction are obtained by setting $u_{12}=v_{12}=v_2=0$ so that we have

$$\frac{\partial u_0}{\partial t} = a - u_0 - \frac{4u_0v_0}{(1+u_0^2)} - \phi, \quad (2.11)$$

$$\frac{\partial v_0}{\partial t} = \sigma b\left[u_0 - \frac{u_0v_0}{(1+u_0^2)} + \phi\right], \quad (2.12)$$

$$\frac{\partial v_1}{\partial t} = -\sigma\left[\frac{bu_0}{(1+u_0^2)} + dk^2\right]v_1. \quad (2.13)$$

Equations (2.11)–(2.13) suggest that the mode responsible for stripe formation, i.e., v_1, is dependent on the dynamics of homogeneous modes. This dependence can be made more explicit by integrating Eq. (2.13) formally for v_1 so that we have

$$v_1(t) = v_1(0)\exp\left[\sigma\int_0^t\left\{-\left(\frac{bu_0(t)}{[1+u_0^2(t)]} + dk^2\right)dt\right\}\right]. \quad (2.14)$$

As the growth of inhomogeneity or its suppression depends critically on the sign of the integral in Eq. (2.14), we show in Fig. 2 the variation in the integral calculated in the long-time limit as a function of ϕ, the illumination intensity. At a critical value of $\phi=3.7$ the integral changes its sign from negative to positive value sharply and one may realize a significant region of positive values of integral approximately in the range $\phi=3.7$–4.3. The region of positive values of the integral corresponds to the growth of v_1 signifying the formation of stripes. This crossover behavior makes an imprint in the variation in steady-state values of v_0 [i.e., $v_{0s}=a(1+u_{0s}^2)/(5u_{0s})$ where $u_{0s}=(a/5-\phi)$ as a function of ϕ]. We observe a divergence of v_{0s} at around $\phi=3.6$ shown in Fig. 3. The consequence of this divergent behavior of v_{0s} is apparent in the numerical simulation which is presented in the latter part of the paper. It is also important to note that the forms of expansion of u and v remain invariant with respect to an interchange in x and y ($k_1=k_2=k$). This symmetry

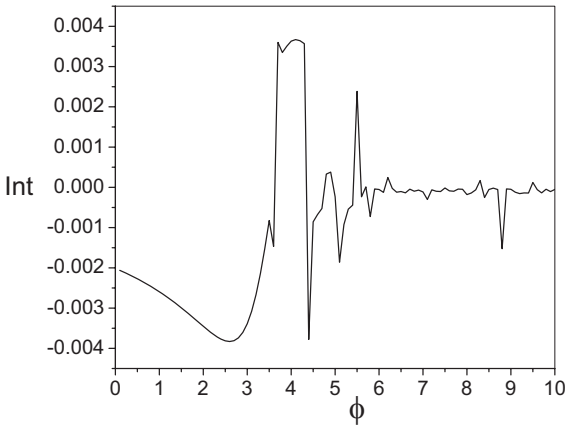

FIG. 2. Variation in integral in Eq. (2.14) as a function of ϕ, the illumination intensity for the given set of parameter values as mentioned in the text.

therefore ensures that stripe along y direction is equally probable as that in x direction provided the choice of nonzero modes are u_0, v_0, and v_2. We thus expect stripes whose components lie both in x and y directions.

We now proceed with the dynamical equations for spot patterns. To this end we set $v_1=v_2=0$ to obtain four-mode equations as follows:

$$\dot{u}_0 = a - u_0 - \frac{4}{1+u_0^2}\left[\left(u_0v_0 + \frac{u_{12}v_{12}}{4}\right)\left(1 - \frac{u_{12}^2}{4(1+u_0^2)}\right) - \frac{u_0u_{12}}{2(1+u_0^2)}(u_0v_{12} + u_{12}v_0) - \frac{5u_{12}^3v_{12}}{64(1+u_0^2)}\right] - \phi, \tag{2.15}$$

$$\dot{v}_0 = \sigma b\left[u_0 - \frac{1}{1+u_0^2}\left\{\left(u_0v_0 + \frac{u_{12}v_{12}}{4}\right)\left(1 - \frac{u_{12}^2}{4(1+u_0^2)}\right) - \frac{u_0u_{12}}{2(1+u_0^2)}(u_0v_{12} + u_{12}v_0) - \frac{5u_{12}^3v_{12}}{64(1+u_0^2)}\right\} + \phi\right], \tag{2.16}$$

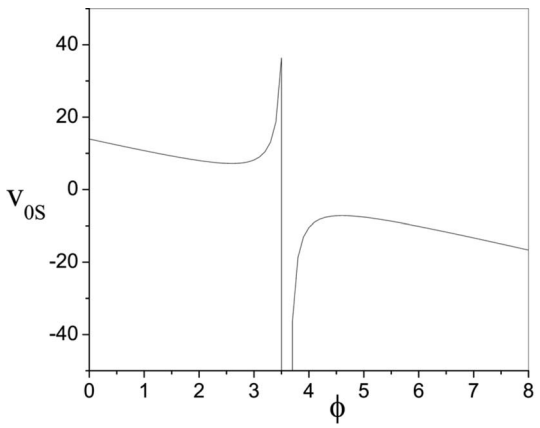

FIG. 3. Variation in v_{0s}, the steady-state values of stripe-mode Eqs. (2.11) and (2.12) as a function of ϕ, the illumination intensity for the given set of parameter values as mentioned in the text.

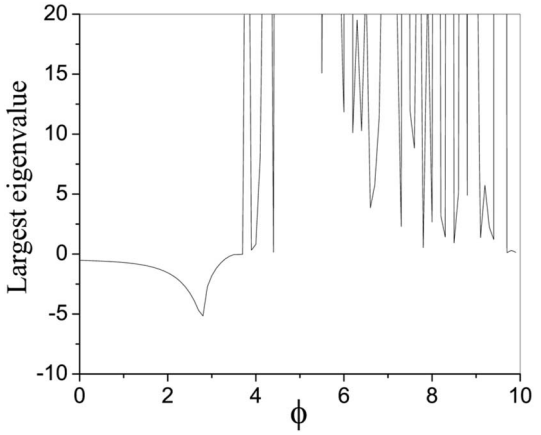

FIG. 4. The plot of largest eigenvalue of the linearized set of equations for the spot-mode Eqs. (2.15)–(2.18) as a function of ϕ for the set of parameter values mentioned in the text.

$$\dot{u}_{12} = -u_{12} - \frac{4}{1+u_0^2}\left[(u_0v_{12} + u_{12}v_0)\left(1 - \frac{u_{12}^2}{4(1+u_0^2)}\right) - \frac{5u_{12}^2}{16(1+u_0^2)}(u_0v_{12} + u_{12}v_0) - \frac{2u_0u_{12}}{(1+u_0^2)}\left(u_0v_0 + \frac{u_{12}v_{12}}{4}\right) - \frac{5u_0u_{12}^2v_{12}}{8(1+u_0^2)}\right] - 2k^2u_{12}, \tag{2.17}$$

$$\dot{v}_{12} = \sigma b\left[u_{12} - \frac{1}{1+u_0^2}\left\{(u_0v_{12} + u_{12}v_0)\left(1 - \frac{u_{12}^2}{4(1+u_0^2)}\right) - \frac{5u_{12}^2}{16(1+u_0^2)}(u_0v_{12} + u_{12}v_0) - \frac{2u_0u_{12}}{(1+u_0^2)}\left(u_0v_0 + \frac{u_{12}v_{12}}{4}\right) - \frac{5u_0u_{12}^2v_{12}}{8(1+u_0^2)}\right\}\right] - 2\sigma dk^2v_{12}. \tag{2.18}$$

The steady-state values of the spot-mode equations u_{0s}, v_{0s}, u_{12s}, and v_{12s} can be obtained numerically. In order to correlate the present analysis with the earlier one we now make a linear stability analysis around this steady state and observe the following points.

(i) For the range of ϕ between 0.0 and 3.6, all the eigenvalues of the stability matrix for the spot-mode equations are negative, implying that the spot state is stable in this region of ϕ values. This is also complementary to the earlier observation in Fig. 2 ensuring suppression of v_1 mode for stripe-mode equation in this region. The negativity of the eigenvalues is demonstrated in Fig. 4 in which the largest eigenvalues have been plotted as a function of ϕ.

(ii) Beyond $\phi=3.6$ the spot steady state becomes unstable since one or more eigenvalues assume positive values. This corresponds to a dynamic changeover of the type of pattern.

(iii) Again for a higher range of ϕ values around 4.4–4.5, the spot state becomes stable.

III. NUMERICAL SIMULATIONS AND DISCUSSIONS

In order to corroborate the above Galerkin analysis with numerical simulations, we carry out numerical integration of

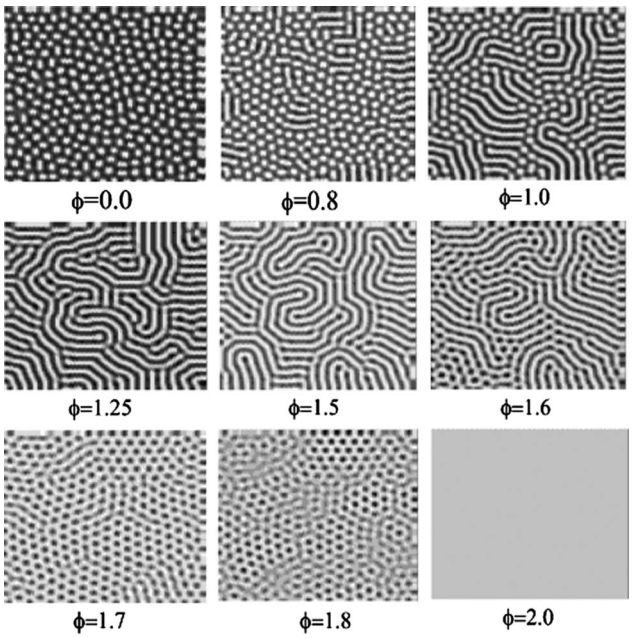

FIG. 5. Turing patterns for different ϕ values, the illumination intensity for the set of parameter values as mentioned in the text.

Eqs. (2.1) and (2.2) in a two-dimensional space. The parameter set chosen for numerical simulation is $a=18.0$, $b=1.5$, $d=1.6$, and $\sigma=9.0$. We use the explicit Euler method for integration of the partial differential equations following discretization of space and time. A finite system size of 100×100 points with zero flux boundary conditions has been chosen. A time interval $\Delta t=0.0005$ and a cell size $\Delta x=\Delta y=1.0$ have been found to be appropriate for this purpose. Turing patterns have been generated by varying illumination intensity ϕ at a fixed initial condition b. The result is shown in Fig. 5. When ϕ is gradually increased from zero, the Turing pattern changes from spot to spot-stripe arrangement and then to stripes. On further increase in ϕ one obtains stripe-spot arrangements which change over to spot. Finally at a high value of ϕ the inhomogeneity disappears altogether corroborating earlier experimental observation [22]. Schematically in Fig. 6, the crossover of the nature of patterns as determined and scaled numerically can be compared to that inferred from earlier Galerkin analysis.

In the Galerkin study of the CDIMA reaction we have analyzed the nature of spatial patterns and their transition from spots to stripes and reverse due to the variation in illumination intensity. The analysis shows that for low intensity the ϕ values for which the spot patterns prevail agree very well to the corresponding range for numerical simulations.

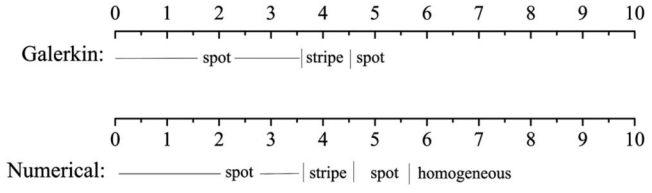

FIG. 6. A comparison between Galerkin and numerical scheme.

The agreement is almost quantitative. However, for higher illumination intensity, the transition of pattern types from spot to stripe and back to spot corroborates the range of ϕ values for numerical simulations well within 5% when compared to the results obtained from Galerkin scheme. For very high ϕ values the nonlinear interaction becomes too severe and one has to consider the excitation of higher harmonic nodes. Thus a four-mode description of spots or a three-mode description of stripes begins to loose its validity. One may, however, take care of larger number of basis functions comprising the contribution of the higher harmonics in addition to the fundamental modes considered for further improvement of the scheme.

A few remarks on the advantage and efficacy of the Galerkin scheme may be in order. It has already been pointed out that amplitude equation technique [1,40] concerns the envelope function of a basic state, and relies on separability of the time scales of the fast and slow modes. It is then possible to eliminate the fast modes which adiabatically follow the slow modes for studying instability in the dynamics. The Galerkin scheme on the other hand, is based on the expansion of the concentration variables in terms of a series of orthogonal basis functions. One can exercise the flexibility by choosing even orthogonal polynomials as basis functions instead of trigonometric functions as employed. Furthermore, no *a priori* separation of time scales of evolution of modes is necessary and all of them are treated on equal footing. Thus in the description of spots and stripes all the four and three modes make their presence felt in the dynamics. Finally a decisive advantage of the scheme in contrast to amplitude equation technique is its extended region of validity beyond near-threshold regime.

IV. CONCLUSION

The Turing instability resulting in initiation of pattern formation is based on linear analysis. However this is always limited by the fact that it is not equipped to deal with the nature of patterns and their crossovers with the variation in parameter space beyond near-threshold regime. One has to go beyond the linear analysis and account for the nonlinear interactions in greater detail. Any analytical treatment is therefore bound to pose considerable difficulty in dealing with this situation. The present treatment relies on the Galerkin technique to analyze a prototypical reaction-diffusion system, CDIMA, which has served as an experimental paradigm for the last two decades. The basic idea is to replace the nonlinear partial differential equations by a set of Lorenz-type ordinary nonlinear differential equations for a few chosen modes. Interesting features of nonlinear dynamics emerge when the number of modes is kept at least three. Our results can be summarized as follows:

(i) We have theoretically analyzed the light-induced Turing patterns and their transition behavior in the chlorine dioxide–iodine–malonic acid system observed by variation in illumination intensity.

(ii) The spot and stripe patterns and their stability can be understood in terms of nonlinear dynamical behavior of a few chosen modes responsible for the specific type of pattern selection.

(iii) The approach emphasizes the conspicuous role of homogeneous mode in relation to other inhomogeneous modes in pattern selection.

(iv) The scope and validity of the present nonlinear analysis extends beyond near-threshold regime.

The Galerkin model is in good agreement with the full-scale numerical simulations and experiments with constant illumination of light intensity. We hope that the method can be extended further to explore the resonant behavior of spatial patterns in presence of periodic and noisy variations in intensity and other related issues.

ACKNOWLEDGMENT

Thanks are due to the Council of Scientific and Industrial Research, Government of India for partial financial support.

[1] M. C. Cross and P. C. Hohenberg, Rev. Mod. Phys. **65**, 851 (1993).
[2] J. Garcia-Ojalvo and J. M. Sancho, *Noise in Spatially Extended Systems* (Springer, New York, 1999).
[3] I. R. Epstein and J. A. Pojman, *An Introduction to Nonlinear Chemical Dynamics: Oscillations, Waves, Patterns and Chaos* (Oxford University Press, New York, 1998).
[4] P. Gray and S. K. Scott, *Chemical Oscillations and Instabilities* (Claredon, Oxford, 1990).
[5] A. M. Turing, Philos. Trans. R. Soc. London, Ser. B **237**, 37 (1952).
[6] H. Meinhardt, *Models of Biological Pattern Formation* (Academic, London, 1982).
[7] V. Castets *et al.*, Phys. Rev. Lett. **64**, 2953 (1990).
[8] Q. Ouyang and H. L. Swinney, Nature (London) **352**, 610 (1991).
[9] I. Lengyel and I. R. Epstein, Acc. Chem. Res. **26**, 235 (1993).
[10] B. Rudovics *et al.*, J. Phys. Chem. A **103**, 1790 (1999).
[11] The chemistry of CIMA and CDIMA is the same at the fundamental level. While the initial input components in the former case are chlorite and iodide, these are ClO_2 and I_2 along with malonic acid in the later version. It has been experimentally observed that after a brief initial period the CDIMA reaction governs the dynamics of pattern formation since ClO_2 and I_2 act as the working reactants. One can therefore measure and control the relevant parameters more directly while working with ClO_2 and I_2 along with malonic acid in CDIMA reaction. See also Ref. [3] for further details.
[12] S Schmidt and P Ortoleva, J. Chem. Phys. **71**, 1010 (1979); **74**, 4488 (1981).
[13] L. Forstova, H. Sevcikova, M. Marek, and J. H. Merkin, J. Phys. Chem. A **104**, 9136 (2000).
[14] L. Forstova, H. Sevcikova, and J. H. Merkin, Phys. Chem. Chem. Phys. **4**, 2236 (2002).
[15] H. Sevcikova and M. Marek, Physica D **9**, 140 (1983).
[16] S. Dutta and D. S. Ray, Phys. Rev. E **73**, 026210 (2006).
[17] S. Dutta and D. S. Ray, Phys. Rev. E **77**, 036202 (2008).
[18] S. Dutta and D. S. Ray, Phys. Rev. E **75**, 016205 (2007).
[19] S. S. Riaz, S. Banerjee, S. Kar, and D. S. Ray, Eur. Phys. J. B **53**, 509 (2006).
[20] A. P. Munuzuri *et al.*, J. Am. Chem. Soc. **121**, 8065 (1999).
[21] A. K. Horvath *et al.*, J. Phys. Chem. A **104**, 5766 (2000).
[22] A. K. Horvath *et al.*, Phys. Rev. Lett. **83**, 2950 (1999).
[23] O. Steinbock, E. Kasper, and S. C. Mueller, Z. Phys. Chem. **216**, 687 (2002); See also, S. C. Mueller *et al.*, in *Nonlinear Dynamics in Polymeric Systems*, ACS Symposium Series No. 869, edited by J. A. Pojman and Q. Tran-Cong-Miyata (American Chemical Society, Washington, DC, 2003).
[24] T. R. Marchant, Proc. R. Soc. London, Ser. A **458**, 873 (2002); A. W. Thornton and T. R. Marchant, Chem. Eng. Sci. **63**, 495 (2008).
[25] M. Dolnik, A. M. Zhabotinsky, and I. R. Epstein, Phys. Rev. E **63**, 026101 (2001).
[26] M. Watzl and A. F. Munster, J. Phys. Chem. **102**, 2540 (1998).
[27] F. Fecher *et al.*, Chem. Phys. Lett. **313**, 205 (1999).
[28] A. Becker and L. Kramer, Phys. Rev. Lett. **73**, 955 (1994).
[29] C. Van den Broeck, J. M. R. Parrondo, J. Armero, and A. Hernandez-Machado, Phys. Rev. E **49**, 2639 (1994).
[30] P. S. Landa, A. A. Zaikin, and L. Schimansky-Geier, Chaos, Solitons Fractals **9**, 1367 (1998).
[31] S. Dutta, S. S. Riaz, and D. S. Ray, Phys. Rev. E **71**, 036216 (2005).
[32] S. S. Riaz, S. Dutta, S. Kar, and D. S. Ray, Eur. Phys. J. B **47**, 255 (2005).
[33] S. S. Riaz, R. Sharma, D. S. Ray, and S. P. Bhattacharrya, J. Chem. Phys. **127**, 064503 (2007).
[34] F. Sagues, J. M. Sancho, and J. Garcia-Ojalvo, Rev. Mod. Phys. **79**, 829 (2007).
[35] V. Petrov, Q. Ouyang, and H. L. Swinney, Nature (London) **388**, 655 (1997).
[36] A. L. Lin *et al.*, Phys. Rev. Lett. **84**, 4240 (2000).
[37] A. Bhattacharyay and J. K. Bhattacharjee, Eur. Phys. J. B **21**, 561 (2001).
[38] L. A. Segel and L. J. Jackson, J. Theor. Biol. **37**, 545 (1972).
[39] E. N. Lorenz, J. Atmos. Sci. **20**, 448 (1963).
[40] A. C. Newell and J. A. Whitehead, J. Fluid Mech. **38**, 279 (1969).